MASTER CONF-790572--3

GCFR FUELS AND MATERIALS PROGRAM AT ARGONNE NATIONAL LABORATORY

by

L.A. NEIMARK, S. GREENBERG, C.E. JOHNSON, A. PUROHIT

Y.Y. LIU, J. REST, K.J. REIMANN AND G.A. McLENNAN

Prepared for

Helium Breeder Associates Review Meeting

San Diego, California

May 30, 1979 - June 1, 1979

U of C-AUA-USDOE

ARGONNE NATIONAL LABORATORY, ARGONNE, ILLINOIS

Operated under Contract W-31-109-Eng-38 for the

U. S. DEPARTMENT OF ENERGY

GCFR FUELS AND MATERIALS PROGRAM AT ARGONNE NATIONAL LABORATORY*

by

L. A. Neimark, S. Greenberg, C. E. Johnson, A. Purohit
Y. Y. Liu, J. Rest, K. J. Reimann, and G. A. McLennan

ARGONNE NATIONAL LABORATORY
Argonne, Illinois 60439

ABSTRACT

The objective of the Argonne National Laboratory Fuels and Materials Program is to develop the additional materials technology, beyond that being generated for the LMFBR, necessary for the development and design of a helium-cooled fast-reactor core using vented and helically ribbed fuel pins.

The F-5 fuel-pin irradiation experiment in EBR-II is a cornerstone of the GCFR program. It is the largest-scale fuel-pin experiment in the present program and will provide data on the performance of pins and a pin-support structure that are prototypic of the GCFR Demonstration Plant. The fuel pins are presently undergoing interim examination after successfully achieving 4.6 at. % burnup. Studies of the thermodynamics and kinetics of the U-Cs-O system, supplemented by analysis of the results of previously irradiated fuel pins, have led to the incorporation of fuel-design modifications in the F-5 experiment to insure adequate performance of the vented fuel.

The effect of ribbing, as well as the ribbing process, on the short- and long-term structural performance of fuel-pin cladding is being evaluated via in-reactor and out-of-reactor tests and with the fuel-element modeling code LIFE-GCFR and the finite element program, ADINA. The results to date indicate that ribbing is not detrimental to cladding performance. NDE methods are being developed to insure the adequacy of commercially ribbed tubing for the Demonstration Plant.

The effects of various fuel-management strategies on structural performance of a downflow core have been evaluated analytically.

The impact of the decision in favor of an upflow core on the ANL development program is being evaluated. At this time it appears the greatest effect will be in the area of core structural performance.

INTRODUCTION

The helium-cooled and vented fuel pin for the GCFR requires surface-roughened cladding and must operate with a small pressure differential across the cladding, in an impure helium environment (containing hydrogen and water vapor) which communicates with the internal helium bond. Achieving these objectives requires a technology beyond that being developed for LMFBR mixed-oxide fuel pins. The objective of the Argonne National Laboratory (ANL) Fuels

---

*Work supported by the U. S. Department of Energy.

and Materials Program is to contribute to the development of the required technology. Specifically, the areas of effort comprise the fuel and cladding, the fuel pin, and the fuel and blanket elements. The purpose of the work is to evaluate the performance of the materials and components under conditions that are as close to prototypic as possible. Since completely prototypic conditions cannot be achieved and some types of experimental work cannot be performed at all, the experimental program is supplemented by an analytical program in order to develop the necessary predictive capability required for design of the GCFR Demonstration Plant.

The ANL Fuels and Materials Program is a coordinated multidisciplinary effort and includes close cooperation with General Atomic Co. (GA). The effort at ANL is organized into subtasks, as shown in Table 1. The specific objectives, accomplishments and future plans are discussed for five of these subtasks in the following review.

TECHNICAL PROGRAMS

I. Fuel-pin Performance*

The objective of the Fuel-pin Performance task is to obtain fuel, blanket, and fuel-pin performance data from in-reactor experiments, to establish a data base for reliable GCFR fuel-pin design and performance. Irradiations of mixed-oxide fuel pins have been performed in thermal and fast reactors, and analytical modeling efforts are in progress to help evaluate current and past experiments and to aid in the analysis of the Demonstration Plant reference fuel pin.

This task is closely associated with the Postirradiation Examination task, from which the experimental data are derived.

a. Thermal-flux Irradiations

GA experiments GB-9 and GB-10 each consisted of encapsulated vented single fuel pins.† They were irradiated in the Oak Ridge Research Reactor to burnups of $\sim$5 and $\sim$10 at. %, respectively. GB-10 differed from GB-9 in that it utilized ribbed rather than smooth fuel cladding, and incorporated provisions for sampling and measurement of the gas flow through the various regions of the pin, and the capacity for on-line measurement of tritium release. The PIE of the fuel pins was accomplished at ANL and has been reported elsewhere.[1,2]

To summarize the findings, volatile fission products migrated to the ends of the fuel columns, and in the case of GB-10, cesium reaction with the bottom UO_2 insulator pellet resulted in the development of a flow blockage at power, i.e. flow was less than the lowest limit of detection, 8×10^{-4} mL/s.

---

*Includes Subtasks B and F.
†The fuel pins and capsules were fabricated at ORNL; ANL was Experiment Manager for GB-10.

Table 1

ANL FUELS AND MATERIALS PROGRAM

Subtask	Principal Investigator
(A) Fuel-pin Fabrication[1]	H. R. Thresh, Materials Science Division
(B) Fuel-pin Performance	L. A. Neimark, Materials Science Division
(D) Materials Properties	W. J. Shack, Materials Science Division
(E) Fuel and Cladding Chemistry	C. E. Johnson, Chemical Engineering Division
(F) Postirradiation Examination	L. A. Neimark, Materials Science Division
(G) Core Design Technology	G. A. McLennan, Components Technology Division

[1] This subtask is not active at the present time. When active, it provides fuel-pin fabrication services for the in-reactor experimental program.

Fission-product attack on the cladding occurred to a depth of <5 mils at the ~720°C maximum cladding-ID temperature of the fueled region in both experiments. In agreement with mechanical-property studies reported in a later section, the ribs appeared to have a strengthening effect on the cladding.

b. Fast-flux Irradiations

Three fast-flux irradiation experiments* have been carried out or are in progress in EBR-II. F-1 and F-3 were GA experiments for which the PIE of the fuel pins was accomplished at ANL.[3,4,5] The F-5 experiment is an ongoing ANL experiment in close cooperation with GA.

The F-1 experiment consisted of 13 encapsulated pins successfully irradiated in three segments to a maximum burnup of 13.6 at. % in the lead pin. The irradiation conditions and results are summarized in Table 2. As was the case for the thermal-flux irradiations, and for most oxide fuel pin irradiations in EBR-II, fission-product cesium migrated to the ends of the fuel columns. However, for at least two pins, G-8 and G-9, there is evidence that a blockage, probably at the fuel/blanket interface, trapped fission gases in the fuel region. The pressure-equalization system, an essential component of the GCFR fuel pin, cannot function properly if fission gas is prevented from reaching the plenum. Unexpected central fuel melting occurred in at least two pins, G-1 and G-2. A possible cause of the melting is a decrease in the fuel thermal conductivity due to the accumulation of gaseous fission products in the fuel, as was concluded for the GE F20 experiment.[6] However, most of the higher-burnup pins in the F-1 series showed no evidence of melting, so that a definitive conclusion is not in hand. The cladding diameter and density measurements indicate that fuel-cladding mechanical interaction can be expected in the vented GCFR fuel pin.

The F-3 experiment consisted of ten encapsulated ribbed-cladding, mixed-oxide fuel pins. Nine of the pins were found to have failed (and the tenth appeared on the verge of failure) at an interim examination after ~5 at. % burnup. Destructive examination of the unfailed pin and reexamination of an unirradiated sibling capsule led to the conclusion that failure resulted from inadequate pin-capsule bonding and was in no way related to fuel-pin design or performance. The F-3 experiment thus became irrelevant to the GCFR program.

The F-5 irradiation experiment[7] is the largest-scale fuel-pin experiment in the present GCFR program. Approximately 35 unencapsulated helically-ribbed mixed-oxide fuel pins are being subjected to several irradiations in the EBR-II. The experiment will provide data on the performance of pins and a pin-support structure that are prototypic of the GCFR Demonstration Plant designs. The pin diameter is 7.46 mm and the cladding thickness is 0.38 mm at the rib root. The rib height is 0.13 mm and the helical pitch is 1.56 mm. The peak BOL linear power rating is 12.3 kW/m and the maximum cladding ID surface temperature is nominally 715°C. Studies of the

---

*The fuel pins and capsules for F-1 were fabricated at ORNL; those for F-3 were fabricated at ANL. The fuel pins for F-5 were fabricated at HEDL.

Table 2
IRRADIATION CONDITIONS AND RESULTS FOR GCFR EXPERIMENT F-1

	Fuel Characteristics		Irradiation Conditions				Fission-gas Release		ΔD/D, %			
										Amount Attributed to		
Element	O/M[a]	Smeared Density, % Theor.	Max. Cladding ID Temp., °C	Peak Linear Heat Gen., W/cm	Burnup,[b] at. %	Fluence, $n/cm^2 \times 10^{22}$	mL (STP)	As Percent of Total Amount Generated[b]	Max. Measured	Swelling[c]	Plenum Pressure	FCMI
G1	1.992	82.6	760	491	5.6	3.88	117	90	0.20	0-0.04	0.02	∿0.17
G2	1.971	84.1	725	473	5.4	3.62	112	88	0.10	0-0.01	0.02	∿0.07
G3	1.987	85.5	695	473	2.8	2.06	39	64	0.20	0-0.01	0.01	∿0.18
G4	1.983	82.5	680	456	13.6	9.69	294	87	0.51	0.01-0.41	0.14	0-0.35
G5	1.990	83.5	640	437	5.1	3.39	not measured		0.13	0-0.02	0.02	∿0.10
G6	1.972	82.7	685	440	5.1	3.26	64[d]	55[d]	0.07	0-0.01	0.02	∿0.05
G7	1.984	82.5	570	420	5.1	3.42	not measured		0.07	0-0.06	0.02	0-0.05
G8	1.985	86.0	672	486	11.5	8.32	176[e]	66[e]	0.72	0-0.40	0.07	0.22-0.62
G9	1.947	84.6	727	480	8.9	5.96	133[f]	64[f]	0.22	0-0.03	0.06	∿0.14
G10[g]	1.968	84.2	727	480	9.8	6.42	160	75	0.19	0-0.03	0.07	∿0.10
G11[g]	1.968	84.3	729	504	9.6	6.87	174[h]	80[h]	0.24	0-0.07	0.07	0.10-0.17
G12[i]	1.976	84.3	735	454	9.7	5.88	157[j]	76[j]	0.38	0-0.03	0.05	∿0.30
G13[i]	1.973	84.4	772	504	9.5	6.96	175	79	0.52	0-0.03	0.06	∿0.40

[a] As-fabricated ratio of oxygen to heavy-metal atoms.

[b] From chemical analysis of burnup samples.

[c] These values were calculated using the equation from the Nuclear Systems Materials Handbook recommended for 20% cold-worked N-lot Type 316 stainless steel, the cladding material for these elements. Measurements of cladding density indicated that within the experimental error of the procedure there was no irradiation-induced change in density.

[d] May be low because of adsorption on active trap.

[e] Of this quantity, 11 mL (4% of the total fission-gas generated) was released from the bottom plenum and 160 mL (60%) from the top plenum in a burst after handling.

[f] Includes ∿86 mL (Kr + Xe), or 41% of the total amount generated, released upon cutting into the upper blanket region of the element.

[g] Ribbed cladding on fuel element; all others smooth cladding.

[h] A negligible quantity of fission gas was released upon drilling into the fuel region.

[i] Solid fuel pellets; all others annular.

[j] 6.1 mL of fission gas (∿3% of that produced) was released upon heating the lower trap. Negligible quantities of fission gas were released upon heating the upper trap and fuel and upon drilling into the fuel.

thermodynamics and kinetics of the U-Cs-O system, supplemented by analysis of the results of previously irradiated fuel pins, have led to the incorporation of low-density blanket material adjacent to the ends of some of the fuel columns to evaluate this potential remedy for the cesium-urania reaction, and thus insure the viability of the vented fuel-pin concept. The experiment is presently undergoing interim examination after successfully achieving 4.6 at. % burnup.

Disassembly was successfully completed with no damage to the fuel pins in spite of a maximum bow of $\sim$2.5 cm in the pins subjected to the greatest thermal gradient. Subassembly profilometry data and fuel-pin gamma spectroscopy data are being evaluated. Neutron radiography of the loaded subassembly as well as of the individual pins showed no unexpected changes in fuel or trap structure. Figure 1 is a photograph of the subassembly after removal of the hex can.

The current plan for the F-5 experiment includes fission-gas depressurization and resealing after this interim examination, followed successively by a step decrease and a step increase in order to simulate subassembly rotation in the unrestrained downflow core. However, now that the GCFR Demonstration Plant will likely use a restrained upflow core, subassembly rotation may not be a part of the fuel-management scheme and consideration is being given to revising the experiment plan. It should be noted that the remote depressurization and resealing of irradiated fuel pins, while a difficult and challenging operation, is specific to the F-5 experiment and not an intrinsic part of the GCFR concept.

The need for larger-scale irradiation tests in the Fast Flux Test Facility remains an open question. Such experiments, albeit in flowing sodium, would be more prototypic than any other experiments in the present program in the areas of fuel length, axial power distribution, fluence/burnup ratio, bottom plenum (to simulate bottom venting in an upflow core), pin-support behavior, bundle-duct interaction, and duct behavior. A limited number of in-core subassembly tests would increase the dedicated GCFR fuel-pin data base by at least a factor of three. The need for these experiments would be even more pressing should the GCFR program select a cladding material not currently being emphasized in the LMFBR advanced oxide program.

c. Fuel-performance Analysis

The objective of the analytical modeling effort is to evaluate the steady-state and transient performance of GCFR fuel pins for the determination of performance characteristics, operating limits, and design criteria. To this end, analytical tools such as the LIFE code are being adapted and/or developed and applied to the anlaysis of GCFR prototypic and experimental fuel rods. Support is also given to pretest planning and posttest interpretation of results.

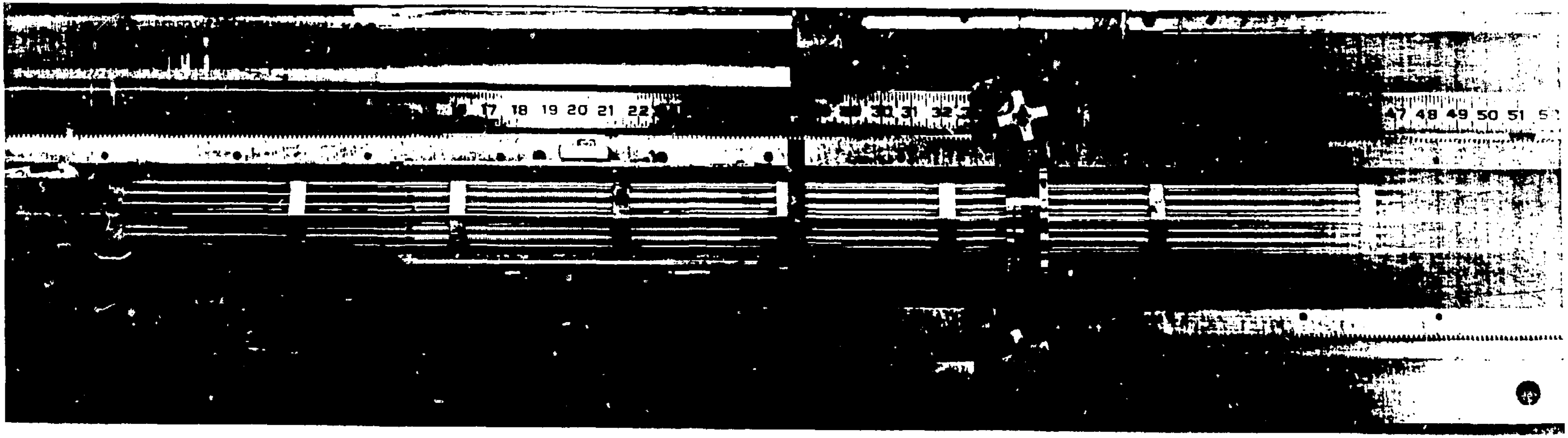

Fig. 1. Partially Disassembled F-5 Experiment.

Several modifications have been made in the LIFE-III mixed-oxide fuel-performance code in order to incorporate certain unique features inherent in GCFR fuel-pin design. For example, sodium coolant properties have been replaced by those of helium gas, and separate Nusselt number correlations for helium gas flow have been adopted to account for the difference in heat-transfer characteristics along the smooth and ribbed portions of the cladding. The pressure-equalization system can be modeled with the modified LIFE code by setting the plenum pressure at a constant level of ∿9.0 MPa (1280 psi) and varying the thermal conductivity of the fuel-cladding gap to reflect degradation of gap conductivity resulting from released fission gases.

An assessment of GCFR cladding stresses (utilizing the GCFR version of LIFE) caused by various primary and secondary loadings during irradiation has recently been completed.[9] Reference power histories for steady-state, step power-change and power-cycling operations were investigated for the downflow core. The largest fuel-cladding interfacial pressure buildup during fuel-cladding mechanical interaction occurs in the step power-change case, but the resulting cladding stresses are still considerably below the cladding yield stress and should not impose any serious threat of cladding failure.

The fuel and cladding behavior models in LIFE will be improved and refined as the work progresses. Work has already started to replace the current semiempirical models of fission-gas release and fuel swelling in LIFE-III by the mechanistic model GRASS-SST[10] and its fast-running version, FASTGRASS.[11] After the replacement is made, the code will be used to study reference GCFR operating conditions.

II. Materials Properties*

The objective of the Materials Properties task is to determine the mechanical properties and behavior of ribbed cladding (including advanced alloys) in impure helium environments and to develop methods to nondestructively qualify ribbed tubing for the GCFR Demonstration Plant.

The basic materials properties required for GCFR core design are expected to be determined through the LMFBR R&D program. However, additional data are required for a complete and safe design of the GCFR core, including fuel elements, due to operating differences between the two reactor types. The GCFR materials-properties R&D program conducted jointly by ANL and GA has identified three specific program objectives based on the need for additional data in the following areas: (a) The effect of ribbed geometry and rib fabrication technique on the mechanical behavior of fuel cladding under various states of stress, (b) the oxidation kinetics of the 20% CW Type 316 stainless steel and advanced alloys proposed as cladding materials, and (c) the chemical (oxidizing/reducing species) effects of the GCFR environment on the mechanical properties. (a) and (b) are discussed below.

---

*Subtask D.

a. Effect of Ribbed Gemoetry and Rib Fabrication Technique

Biaxial creep-rupture tests ANL-I through III,(12-14) involving a total of about one hundred specimens, have been completed. Tests ANL-I and II were performed under high oxidizing potential (P_{O_2} = 21 Pa), while ANL-III was performed under the tentative prototypic GCFR environment (H_2 and H_2O partial pressures of 3000 and 300 Pa, respectively, in a total system pressure of 1 MPa). All three tests were performed at the nominal maximum GCFR operating temperature of 650°C. The results indicate that ribs fabricated by an electrochemical etching process is not detrimental to the mechanical strength, while mechanically ground ribs in fact impart about 10% additional strength to the cladding. These tests also indicate that the environment investigated is an acceptable operating environment from the point of view of cladding strength and durability.

Tests of 15 previously irradiated electrochemically etched ribbed and mechanically ground smooth specimens have been completed.(15) These specimens were tested under a hoop to axial stress ratio of either 2:1 (internally pressurized) or 1:1 (internally pressurized and also axially loaded). The test results indicate that the postirradiation biaxial creep-rupture strength of the electrochemically etched cladding is not affected by the ribbed geometry. These results are significant, since the electrochemical etching process is still in the early stage of development and the ribs fabricated by this method to date have contained numerous large and small defects. Such defects have been shown to be the nucleation sites for the failure cracks.(12,13)

The design of the test matrix and the required specimen fabrication for the unirradiated ANL-IV test have been completed. At the conclusion of this test series we will be able to determine the effect of an oxidizing GCFR environment with an H_2 and H_2O partial pressures of 100 and 400 Pa, respectively. The actual test series will begin in July 1979 and be completed by July 1980. The test temperature is 650°C. The proposed test temperature for ANL-V is 700°C, corresponding to the "hot-spot" temperature for the fuel cladding. Future tests may involve cyclically varying the oxidation potential. The detailed justifications for such tests depend to a large degree on the results of tests ANL-III to -V and on the oxidation tests that are in progress at GA.

In another series of tests, uniaxial tensile data for ribbed and smooth cladding were compared at 650°C. Results have been obtained for smooth specimens from two heats of 20% CW Type 316 stainless steel and mechanically ground ribbed specimens from one of these heats. No heat-to-heat variation was observed for the smooth specimens. The results for the ribbed specimens indicated that (a) most of the specimen strain occurs in the root region, (b) the root-radius region is not a stress raiser, and (c) the rib section contributes its full geometrical share to the load-bearing capacity of the cladding.

Additional tests of specimens fabricated by means of electrochemical etching and electrochemical grinding are in progress.

b. Oxidation-kinetics Study

This study is being jointly conducted at GA and ANL. The basic oxidation measurements and oxide morphological studies are being carried out by Acharya and Langer[16] at GA. The chemistry and elemental distributions of the oxides are being investigated at ANL using Auger electron spectroscopy coupled with an ion-etching technique. In addition to the candidate cladding alloy, 20% CW Type 316 stainless steel, all the advanced alloys under consideration for use in the LMFBR program have been included in this oxidation study.

To date, specimens have been exposed for 5000 h to a 1-MPa helium environment containing H_2 and H_2O partial pressures of 3000 and 300 Pa, respectively. The results indicate that the oxide on all mechanically ground or as-drawn specimens is primarily Cr_2O_3. If the base alloy contains manganese and/or titanium, the oxide on mechanically ground surfaces is enriched in these elements by a factor of ∿10. The phenomenological implication of the observation of chromium-, manganese- and titanium-rich oxide is that the growth kinetics of the oxide are controlled by cation diffusivity. These observations are also supported by the work of Hagel and Seybolt.[17] The practical implication of this finding for the operation of a GCFR is very significant. Oxidation rate and consequent effects on mechanical properties are independent of oxidation potential over a relatively wide range (conservatively, on the order of a factor of 100). Additional details regarding the oxidation test results are given by Acharya, Langer, and Purohit[18] and by Purohit.[19]

In summary, the information obtained to date on the properties of ribbed CW Type 316 stainless steel cladding shows that:

(a) Ribs are not detrimental to the biaxial (2:1 and 1:1) creep-rupture and uniaxial tensile strength of the cladding.

(b) Ribs produced by mechanical grinding appear to increase the strength of the cladding by ∿10% as compared with that of smooth cladding equal in thickness to the root region of the ribbed cladding.

(c) The oxide formed on mechanically ground or as-drawn cladding exposed at 650°C to 1/MPa of helium gas containing 3000 Pa H_2 and 300 Pa H_2O is chromium-rich. No detrimental effect on cladding performance is expected from fairly large changes (by a factor of at least 100) in the oxidation potential.

The following additional work is planned to demonstrate that ribbed tubing adequate for GCFR service can be produced economically:

(a) Investigation of the effects of flow-induced low-amplitude, high-frequency vibrations. The mechanical damage induced by these vibrations is of two types:

(1) classical corrosion-fatigue damage, and

(2) wear and fretting-type damage due to particulate matter contained in the coolant gas and/or to friction between the cladding OD surface and the grid support plate.

(b) In-reactor mechanical testing of GCFR cladding fabricated from advanced alloys and 20% CW stainless steel.

(c) Continuation of out-of-pile mechanical tests to determine the effects of various combinations of temperatures and oxidation potentials at relevant stress biaxialities.

(d) Study of the effect of irradiation on the corrosion of GCFR candidate materials.

(e) Development of an economical rib-fabrication technique via a two-step process involving sequential electrochemical and mechanical or chemical polishing processes.

d. Cladding Behavior Analysis

The mechanical behavior of ribbed GCFR cladding under multiaxial loading conditions will be analyzed using the finite element code ADINA.[19] This code has both two-dimensional and three-dimensional analysis capabilities for nonlinear material behavior and large deformation. Initially, a two-dimensional analysis will be performed on ribbed cladding with 2:1 and 1:1 stress biaxiality. The results will provide direct input to the multiaxial creep-rupture tests now in progress as part of the cladding development program at ANL.

Analysis of the swelling-induced cladding stresses indicates that a stress reversal can occur depending upon the nature of the cladding swelling gradient.[20] The cladding swelling gradient will be either in phase with or opposite to the cladding temperature gradient when the cladding temperatures are, respectively, below or above the peak swelling temperature for the 20% cold-worked 316 stainless steel. If the cladding temperatures swing back and forth across this peak swelling temperature during operation, both the temperature cycles and the swelling cycles can be expected to contribute to a fatigue-type loading on the cladding.

e. Nondestructive Examination

Adaptations of standard nondestructive inspection methods are necessary for the production-scale qualification of ribbed cladding. Several techniques were evaluated for wall-thickness measurement and integrity assessment; pulsed eddy-current inspection with point probes was shown to be capable of measuring wall thickness to the desired accuracy and detecting artificial flaws. High inspection speeds for wall-thickness measurement and flaw detection will require modification of the existing pulsed eddy-current coils; circumferential coils requiring only a single pass are presently being evaluated. An air-gauging system, the KWR system, "tally-surf", and optical comparators were evaluated for rib-geometry measurements; the use of an electro-optical system is contemplated. After finalization of the cladding design, an integrated inspection system comprising pulsed eddy-current equipment and a computerized comparator with the necessary drive system will be built in cooperation with commercial vendors.

III. Fuel and Cladding Chemistry*

The objective of the Fuel and Cladding Chemistry task is to identify significant problem areas relating to the vented fuel system and to develop design and operational specifications to alleviate the problems. The vented and pressure-equalized fuel pins[22] for the GCFR must operate in a helium environment containing relatively high concentrations of water vapor and hydrogen.[23] This is the unavoidable consequence of direct contact between the primary coolant and the steam generator. Meeting these conditions of GCFR fuels and materials operation requires a comprehensive understanding of the fuel-fission product chemistry in a GCFR fuel pin.

A vented GCFR fuel pin can be successfully operated only as long as axial gas-transport paths are available and operating within the pin. However, axial gas-flow restrictions have been observed in GCFR test pins and attributed to the formation of a low-density Cs-Uo-O compound at the interface between the mixed-oxide fuel and the uranium oxide blanket. With the formation of such a compound(s), flow restriction may occur because of the large difference in molar volume between urania and the Cs-U-O compounds. To aid in understanding this plugging phenomenon, work at ANL has focused on identifying the Cs-U-O phase that forms,[22] identifying the thermodynamic and kinetic constraints governing a flow-blockage situation,[23] and designing a means of eliminating flow restrictions in future GCFR fuel pins.[24] The Cs-U-O phase that forms under the conditions expected at the fuel-blanket interface is Cs_2UO_4.[22,23] At lower than expected temperatures and/or higher than expected oxygen potentials ($\Delta\bar{G}_{O_2} = RT \ln p_{O_2}$), $Cs_2U_4O_{12}$ forms and causes 70% more swelling than Cs_2UO_4. The thermodynamic boundary condition for the formation of cesium uranate is dictated by the activities of cesium and oxygen, according to the reaction

$$2Cs(g) + UO_2 + 2\ O\ (\text{in } UO_{2-x}) \rightarrow Cs_2UO_4.$$

The limiting kinetic constraint[24] is the rate of cesium transport to the urania blanket. Thus, laboratory data are in accord with in-reactor results; i.e., cesium reacts rapidly with the first few blanket pellets and does not accumulate in the entire blanket. This knowledge was used in designing a means of accommodating the formation of low-density cesium uranate in GCFR fuel pins. The plan, currently being tested in the F-5 experiment in EBR-II, is to provide sufficient voidage within the first few blanket pellets so that axial gas-flow paths are not seriously restricted by the swelling accompanying the formation of a cesium uranate.

Future work will focus on extrapolating the existing data base on cesium migration (in short, EBR-II-type pins with a fuel section of 34 cm) to predict behavior in prototypical GCFR pins with a 1-m-long fuel section. Because of the different axial temperature gradients, oxygen (and therefore cesium) may accumulate within the 1-m fuel section, not at the urania blanket/fuel interface. In addition, future work will focus on identifying the migrating cesium species. The difference between Cs(g) and CsOH(g) as the migrating species is significant because cesium and oxygen comigrate in the latter case, but not the

---

*Subtask E.

former, and the presence of oxygen will affect the reaction thermodynamics. Additional work will focus on assessing the impact of cladding breach and the accompanying influx of hydrogen and moisture impurities on the potential for flow restriction in a GCFR fuel pin.

The high hydrogen levels in the helium coolant (and also in the fuel pin, via diffusion through the cladding) increase the probability for the condensation of extremely corrosive liquid CsOH on the cladding inner surface.(25,26) Such a condition may lead to a breach of the cladding. A model of fuel-cladding chemical interaction processes has been developed which correctly predicts LMFBR results; according to this model, the depth of cladding attack will increase with increasing hydrogen level. Future work in this area may focus on exploiting the existing LMFBR data base to assess limitations on fuel-pin performance in the presence of high hydrogen levels.

IV. Core Design Technology*

The objective of the Core Design Technology task is to assure the adequacy of GCFR design and operational strategy in accommodating radiation-induced swelling and radiation-enhanced creep of stainless steel and advanced alloys. thermal gradient- and radiation-induced bowing of fuel elements, and seismic events. To date, the core design effort for the GCFR program has focused on studies of core-assembly bowing and dynamic seismic response, both based on the original unrestrained-downflow concept.

Core structural analysis, which included the effects of duct dilation and bowing due to thermal gradients and irradiation-induced swelling and creep, have been performed. Initial two-dimensional studies (for radial spokes of assemblies) were conducted for several different refueling schemes. The primary conclusion from these two-dimensional studies was that assembly interactions could be significantly reduced, or eliminated, by selective duct rotations during refueling. Subsequent three-dimensional studies (for a 60° sector of assemblies) were performed in an attempt to establish that the two-dimensional model and conclusions were adequate.

Figures 2 and 3 show some comparisons of the end-to-end contact forces for two radial spokes of assemblies, as obtained from the 2-D and 3-D analyses, for a refueling scheme with no duct rotations. These results are for the third cycle (500-750 days) for a core of originally straight assemblies. In these figures, P_i represents the radially inward force acting on the downstream end of the assembly in row i. At equilibrium, P_i is equal and opposite to the radially outward force Q_{i+1} acting on the end of the assembly in row i+1. As indicated, the 2-D and 3-D results differ quantitatively, with considerably lower forces and later contact times predicted by the 3-D model. These differences have been attributed to differences between the 2-D and 3-D codes in the modeling of temperature and flux gradients, resulting in less thermal bow and additional creep relaxation in the 3-D model.

---

*Subtask G.

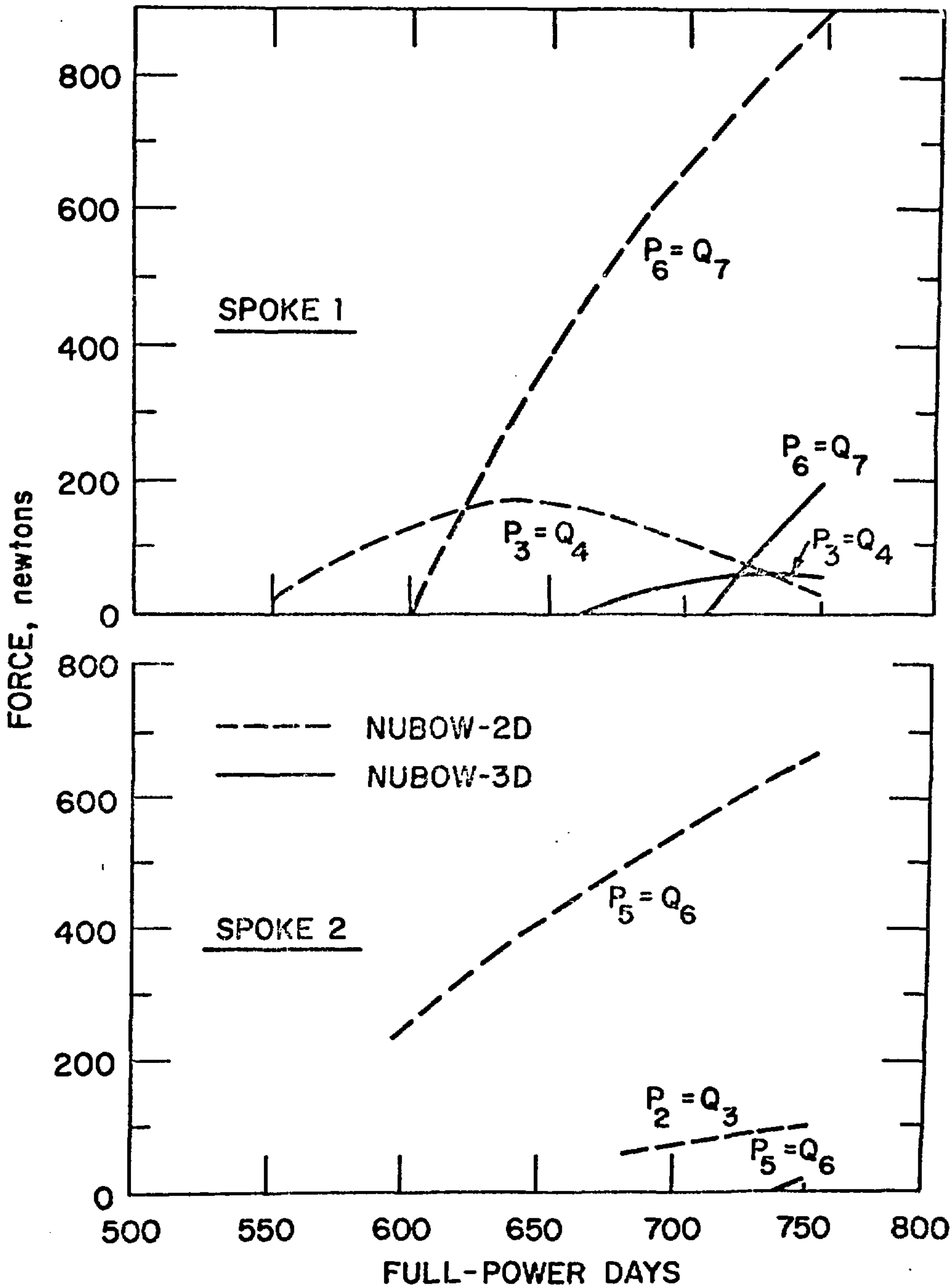

Fig. 2-3. Comparison of NUBOW-2D and NUBOW-3D Duct Interaction Forces (Third Cycle, No Duct Rotation).

Although quantitative differences in force levels were noted between the 3-D and 2-D results, no major 3-D geometric effects were observed. Figure 4 shows the 3-D contact state for the same case shown in Figs. 2 and 3 at the end of 750 days. The numbers in the subassembly hexagons refer to the loading cycle. For the assemblies which lie off the radial spokes, contacts did occur, in a pattern reflecting the change from Spoke 1 to Spoke 2, and with comparable force levels.

As part of the three-dimensional calculations, the material-properties correlations for creep and swelling were updated to reflect the latest revision in the Nuclear Systems Materials Handbook. These revised relationships predict considerably more creep and swelling, and as a consequence, the calculated results showed significantly more duct-to-duct end interaction and dilation contact near mid-core. The basic conclusion drawn from these results was that for the revised material correlations, duct-to-duct interaction would have to be accommodated in an unrestrained GCFR core.

Dynamic seismic-response studies have been directed to the analysis of single-assembly response and impacts between adjacent assemblies in small clusters (e.g., seven assemblies). Preliminary results indicate that duct impacts will occur during a seismic event and that the nature of these impacts is quite complex. Impact-force magnitude and oscillation period have been shown to be dependent on duct-to-duct gap size and damping. This dependence is chaotic because of the nonlinearity of the dynamic system.

Because of the decision to utilize a restrained upflow GCFR core, core design effort under this task must be reviewed and probably revised. In the area of core structural analysis for the proposed GCFR design, three features which are significantly different from conventional LMFBR technology will be investigated. These are (a) problems due to increased duct dilation, (b) pin-spacer/duct interaction effects, and (c) problems relating to dynamic seismic response which differ significantly from those of the LMFBR because of the lack of fluid inertia and damping effects in the GCFR.

SUMMARY

The ANL Fuels and Materials Program is focused on key areas in the development of the GCFR. The information obtained to date indicates that the unique features of the GCFR, i.e., vented fuel pins, ribbed cladding, and the helium coolant, do not appear to present significant development problems. However, potential changes in materials and fuel-pin design brought about by the need to achieve higher burnups and the recommended change to an upflow core could have significant effects on the development program. The change to an upflow core with bottom-vented fuel pins requires detailed reconsideration of the relevance of existing data. This reconsideration may result in changes in plans for current experiments, e.g., the F-5 irradiation experiment, as well as proposals for new experiments (in-reactor as well as out-of-reactor) or analytical studies, in place of, or in addition to, presently planned efforts.

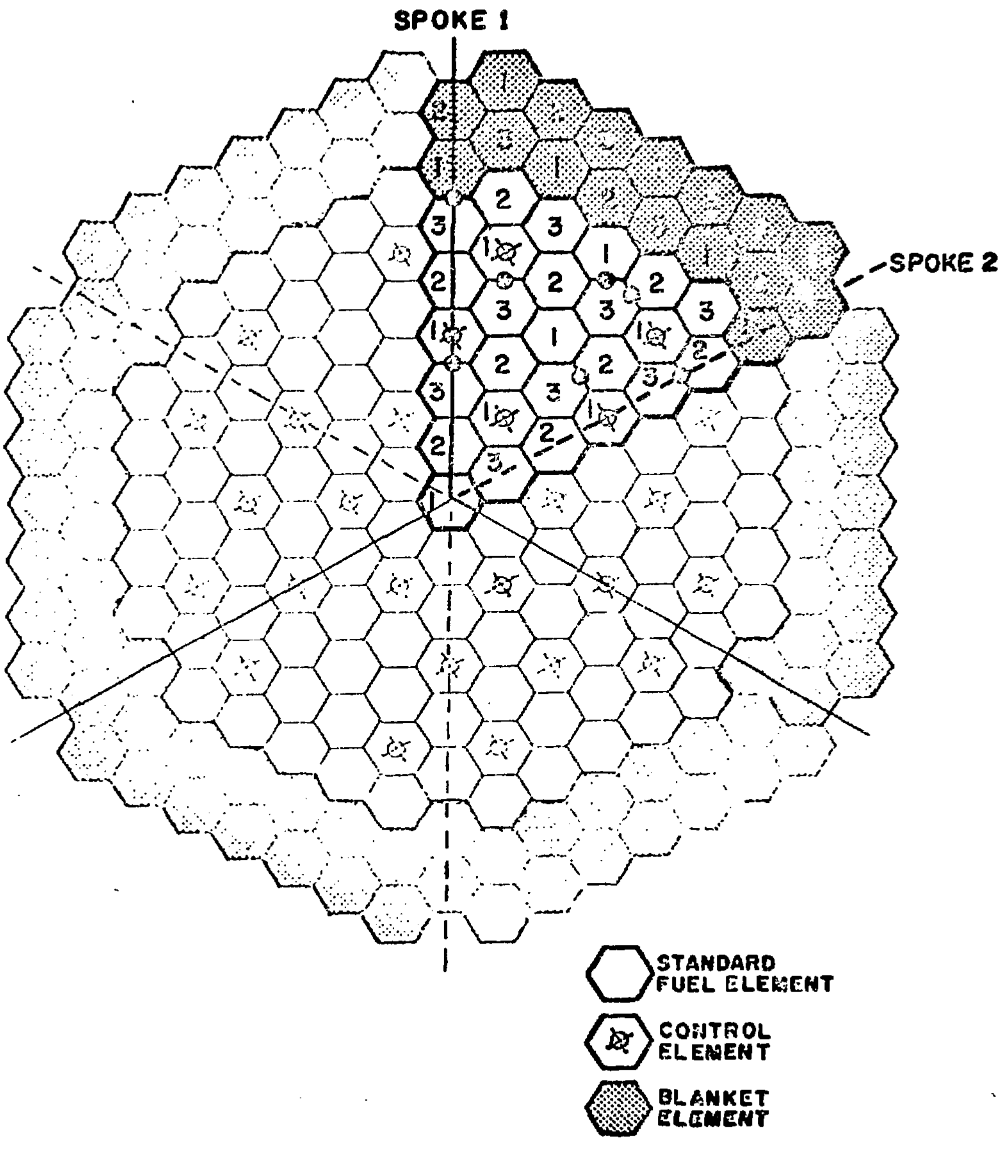

Fig. 4. Calculated 3-D End Contact State at 750 Days (No Rotation).

REFERENCES

1. R. V. Strain, C. W. Renfro, and L. A. Neimark, "Postirradiation Examinations of the GB-9 Element," ANL-8067, Argonne National Laboratory, Oct. 1976.

2. D. L. Johnson, "Postirradiation Examination of the GCFR GB-10 Element," to be published.

3. R. V. Strain, "Postirradiation Examination of Element G-3 from the GCFR F-1 Series of Mixed-Oxide Elements After ~3 at. % Burnup," ANL-76-125, Argonne National Laboratory, Feb. 1977.

4. R. V. Strain and C. E. Johnson, "Postirradiation Examinations of Fuel Pins from the GCFR F-1 Series of Mixed-Oxide Fuel Pins at 5.5 at. % Burnup," ANL-76-129, Argonne National Laboratory, May 1978.

5. S. Greenberg, J. E. Sanecki, and C. E. Johnson, "Postirradiation Examinations of Fuel Pins from the GCFR F-1 Series of Mixed-Oxide Fuel Pins at 13.6 at. % Burnup," in preparation.

6. W. H. McCarthy, D. R. Jedlovec, S. Vaidyanathan, and R. F. Hilbert, "The Influence of Design and Operating Parameters on Mixed-Oxide Fuel Power-to-Melt," Proc. Int. Conf. on Fast Breeder Reactor Fuel Performance, Monterey, CA, March 5-8, 1979, p. 268.

7. D. L. Johnson et al., "Experiment Description and Hazards Analysis: F-5 Series GCFR Mixed-Oxide-Fueled Elements," unpublished work (1977).

8. M. C. Billone et al., "LIFE-III Fuel Element Performance Code," ERDA Report 77-56, Argonne National Laboratory, July 1977.

9. Y. Y. Liu, T. C. Hsieh, and M. C. Billone, "Calculations of Stresses in GCFR Cladding Under Normal Operating Conditions," to be published as an ANL report.

10. J. Rest, "GRASS-SST: A Comprehensive, Mechanistic Model for Prediction of Fission-Gas Behavior in UO_2-Base Fuels During Steady-State and Transient Conditions," NUREG/CR-0202, ANL-78-53, Argonne National Laboratory, June 1978.

11. J. Rest and S. M. Gehl, "The Mechanistic Prediction of Fission-Gas Behavior During In-Cell Transient Heating Tests on LWR Fuel Using the GRASS-SST and FASTGRASS Computer Codes," Proc. 5th Int. Conf. on Structural Mechanics in Reactor Technology, Berlin, Germany, August 13-17, 1979, paper C1/6.

12. F. L. Yaggee, A. Purohit, W. J. Grajek, and R. B. Poeppel, "Biaxial Creep Behavior of Ribbed GCFR Cladding at 650°C in Nominally Pure Helium (99.99%)," ANL-76-73, Argonne National Laboratory, Nov. 1977.

13. A. Purohit, F. L. Yaggee, W. J. Grajek, and W. J. Shack, "Report of Test ANL-II: Biaxial Creep Behavior of Ribbed GCFR Cladding at 650°C," to be published.

14. A. Purohit, W. J. Grajek and L. M. Brydges, "GCFR Creep-Rupture Test ANL-III," in ANL-RDP-71, Argonne National Laboratory, May 1978, pp. 8.1-8.6 and ANL-RDP-80, Argonne National Laboratory, Feb. 1979, pp. 6.1-6.7.

15. A. Purohit, G. L. Fogle, Y. Y. Liu, and R. T. Acharya, "Postirradiation Biaxial Creep-rupture Tests of Ribbed GCFR Cladding," presented at the ANS Annual Meeting, Atlanta, GA, June 3-8, 1979.

16. R. T. Acharya and S. Langer, "Oxidation of SS316 and Advanced Alloy Cladding," GCFR Quarterly Progress Report, Nov. 1, 1978 - Jan 31, 1979, GA-A15237, General Atomic Co., pp. 5-3ff.

17. W. C. Hagel and A. Seybolt, J. Electrochem. Soc. 108, 1146 (1961).

18. R. T. Acharya, S. Langer, and A. Purohit, "Oxidation of SS316 and Advanced Alloy Cladding in GCFR Enrivonment," presented at the ANS Annual Meeting, Atlanta, GA, June 3-8, 1979.

19. A. Purohit, "Oxide Composition of SS316 and Advanced Alloy Cladding in GCFR Environment," to be published.

20. K. J. Bathe, "ADINA, A Finite Element Program for Automatic Dynamic Incremental Nonlinear Analysis," MIT Report 82448-1, May 1977.

21. Y. Y. Liu and T. C. Hsieh, "The Role of Irradiation-Induced Swelling in Cladding Stress Distributions," presented at the ANS Annual Meeting, Atlanta, GA, June 3-8, 1979.

22. D. C. Fee and C. E. Johnson, J. Inorg. Nucl. Chem. 40, 1375 (1978).

23. D. C. Fee and C. E. Johnson, J. Nucl. Mater. 78, 219 (1978).

24. D. C. Fee and C. E. Johnson, unpublished data.

25. D. C. Fee and C. E. Johnson, Proc. Int. Conf. on Fast Breeder Reactor Fuel Performance, Monterey, CA, March 5-8, 1979, p. 372.

26. O. Götzmann, C. E. Johnson and D. C. Fee, J. Nucl. Mater. 74, 68 (1978).